International Journal of Astrobiology 12 (1): 78–86 (2013)
doi:10.1017/S1473550412000444

Adsorption of nucleic acid bases on magnesium oxide (MgO)

Teresa Fornaro, John Robert Brucato, Sergio Branciamore and Amaranta Pucci

INAF – Osservatorio Astrofisico di Arcetri, L.go E. Fermi 5, 50125 Firenze, Italy
e-mail: jbrucato@arcetri.astro.it

Abstract: The adsorption of organic molecules on mineral matrices might have played a fundamental role in processes that led to the emergence of life. We investigated the adsorption properties of the nucleobases adenine, cytosine, uracil and hypoxanthine on magnesium oxide (MgO), determining the single solute batch equilibrium adsorption isotherms. Langmuir-type isotherms were fitted to data, assuming a rapid reversible equilibration of adsorption, demonstrated effectively through desorption experiments. The Langmuir equilibrium adsorption constant K and the amount of the solute per unit of adsorbent mass necessary to complete the monolayer b were calculated. The results indicate that MgO is a good adsorbent for nucleobases (adenine > uracil > hypoxantine > cytosine), suggesting a role of metal oxides in concentrating biomolecules in prebiotic conditions that might have favoured the passage from geochemistry to biochemistry.

Received 20 June 2012, accepted 7 September 2012, first published online 22 October 2012

Key words: nucleobases, magnesium oxide, mineral adsorption, prebiotic chemistry, origin of life.

Introduction

The adsorption of organic molecules on mineral matrices might have played a fundamental role in processes that led to the emergence of life. In the astrobiology context, the interfaces between minerals and aqueous solutions are very interesting because they are dynamic, energetic environments able to selectively adsorb molecules, allowing their concentration, assisting prebiotic self-organization (Bernal 1951; Sowerby *et al.* 1998; Hazen 2006). Minerals can act as catalysts promoting selective synthesis of biomolecules on the surface (Lahav & Chang 1976; Gibbs *et al.* 1980; Sowerby *et al.* 1996, 2002; Ertem 2004; Schoonen *et al.* 2004; Brucato *et al.* 2006; Hazen & Sverjensky 2010; Saladino *et al.* 2011) and, in some cases, their surfaces have also an enantioselective potential and hence a role in the development of chirality in prebiotic conditions (Lahav 1999; Hazen *et al.* 2001; Podlech 2001; Hazen & Sholl 2003; Downs & Hazen 2004; Sholl & Gellman 2009). Moreover, the physico-chemical interactions of biomolecules with the surface of minerals may affect the survival of molecules in space, making them more resistant, favouring their preservation throughout time (Lorenz & Wackernagel 1994; Stotzky *et al.* 1996; Luther *et al.* 1998; Scappini *et al.* 2004), suggesting a pivotal role of minerals in the prebiotic evolution.

In particular, the adsorption of nucleobases, nucleic acid components, on mineral surfaces may have had some prebiotic relevance. The prebiotic availability of these molecules is argued by various studies (Miller 1987; Ferris 1992; Levy *et al.* 2000; Saladino *et al.* 2001, 2003, 2004, 2005a, b; Barks *et al.* 2010). Sowerby and Heckl (1998b) showed that nucleobases adsorb spontaneously at solid–liquid interfaces potentially favouring further prebiotic synthesis and concentrating these molecules even from low yielding reactions. In the case of adenine on molybdenum disulphide (MoS_2), the formation of two enantiomorphous structures of the adenine monolayer suggested a possible path for a prebiotic symmetry breaking (Sowerby *et al.* 1996). According to this it was proposed that a primitive genetic code mechanism would have evolved from prebiotic interactions of racemic amino acids with enantiomorphic monolayers of purine and pyrimidines (Sowerby & Heckl 1998). The study of the adsorption properties of nucleic acid components, such as nucleobases, on mineral surfaces may have important prebiotic implications in the RNA world model of the origin of life (Gilbert 1986; Pucci *et al.* 2010). These scientific investigations are also relevant for supporting life detection space missions such as the ESA ExoMars mission. In fact, the knowledge of the adsorption and desorption thermodynamics of nucleobases on minerals and the investigations on the nature of the interactions between nucleobases and mineral surfaces would allow to identify these molecules as potential bio-markers and hence to develop suitable sample-extraction protocols for bioanalytical instruments (Parnell *et al.* 2007; Cullen & Sims 2008; Peeters *et al.* 2009). The adsorption of nucleic acids to mineral matrices can result in low extraction yields and might negatively influence detection with space robotic instrumentation. Recent study addressed methodological issues to optimize DNA extraction from soils and sediments analogues to terrestrial and Mars minerals (Direito *et al.* 2012). The adsorption of nucleobases has been observed on the surfaces of graphite (Heckl *et al.* 1991; Tao & Shi 1994; Sowerby *et al.* 1996, 2001a, b, 2002 Sowerby & Petersen 1997, 1999; Edelwirth *et al.* 1998;), MoS_2 (Heckl *et al.* 1991; Sowerby *et al.* 1996, 2000; Sowerby &

Petersen 1997, 1999), crystalline gold (Tao *et al.* 1993), rutile (TiO_2) (Cleaves *et al.* 2010), clays (Winter & Zubay 1995; Komiyama *et al.* 1998), pyrite (FeS_2) (Bebié & Schoonen 2000; Cohn *et al.* 2001; Plekan *et al.* 2007), silicon dioxide (SiO_2) (Cohn *et al.* 2001; Plekan *et al.* 2007), pyrrhotite (FeS), magnetite (Fe_3O_4) and forsterite (Mg_2SiO_4) (Cohn *et al.* 2001). We intend to carry out a systematic study on the adsorption of nucleic acid components on other mineral matrices of astrobiological interest, such as metal oxides that are important constituents of the crusts of Earth-like planets and are the first chemical species produced in the cooling stellar outflows. Metal oxides may be involved in processes relevant to the emergence of life on Earth. In fact, they can be strong adsorbants of organic compounds, acting as photo-catalysts in particular conditions (Singh *et al.* 2007). Therefore, the study of the interactions between important biomolecules and metal oxides would be aimed at understanding the possible involvement of such minerals in the chemical evolution of life.

The choice of magnesium oxide (MgO) substrate

The purpose of this work was to investigate the adsorption properties of the nucleobases adenine, cytosine, uracil and hypoxanthine on MgO, one of the metal oxides that have been found on Mars (Ming *et al.* 2006). Furthermore, analysis of Martian meteorite Allan Hills 84001 showed the presence of MgO formed preferentially by precipitation from carbonate as a result of partial decomposition and loss of CO_2 (Barber & Scott 2002). Magnesium is the eighth most abundant element on Earth and a common element also on Earth-like planets. It constitutes about 2% of the Earth crust and is the third element in the marine water. The inorganic chemistry of magnesium may have played a key role in prebiotic geochemistry (Holm 2012). Evidence in support of this hypothesis is the central role of Mg^{2+} in the function of ribozymes, its preserved position in ribosomes, its role in the cellular metabolism, its six-oxygen coordination ability responsible for stabilizing di- and triphosphate groups of nucleotides, assisting the folding of RNA and promoting the formation of nucleobases and carbohydrates such as ribose. Therefore, the study of the adsorption properties of Mg-containing minerals, such as MgO or forsterite, may shed light on the possible involvement of magnesium in prebiotic geochemical processes. In particular, we focused on the thermodynamics of the adsorption process of nucleobases onto MgO, describing the distribution of molecular solute species between the fluid solvent phase and the solid sorbant phase, i.e. the adsorption isotherm at the solid–liquid interface. Models of equilibrium adsorption are based on a hypothesis known as local equilibrium assumption (LEA) (Valocchi 1985), which assumes that, at a microscopic scale, the adsorption process reaches equilibrium instantaneously and, if the concentration in the fluid phase does not change, the adsorbed concentration remains constant. This is possible when, at the microscopic level, the adsorption and desorption rates are much higher than the flow rate of the liquid phase. Among the methods that study the equilibrium adsorption process, there are the phenomenological ones that identify a dependency between the solute adsorbed concentration per unit mass of adsorbent phase and the solute concentration in the liquid phase. At a given temperature the relationship between the degree of surface coverage and the equilibrium solute concentration is the adsorption isotherm: $x/m = f(C)_T$, where x is the amount of solute adsorbed on the solid mass m, C is the solute concentration in the aqueous phase at equilibrium, $f(C)$ indicates a function of the concentration C at the temperature T. We determined the single solute batch equilibrium adsorption isotherms for nucleobases dissolved in water on the surface of MgO at 298 K.

Materials and methods

Adenine hydrochloride 99% and uracil were purchased from Sigma-Aldrich, while cytosine 98 + % and hypoxanthine 99% from Alfa Aesar. Nucleobase stock solutions were prepared by dissolving the appropriate amount of pure nucleobase solids in a specific volume of distilled and sterile water, without modifying the pH. A basic stock solution of hypoxanthine was prepared, due to its low solubility in water at neutral pH. The stock solution pH, measured using a pH 700 Bench Meter Eutech Instruments, was about 3 for adenine, 4 for uracil, 7 for cytosine and 12 for hypoxanthine solutions. The stock solution concentration was accurately determined by UV spectrophotometry using a Varian Cary 50 UV-Vis spectrophotometer. MgO typically 99.5% pure (~325 mesh) was purchased from Cerac and characterized by FT-IR spectroscopy before and after flowing steam sterilization at 120 °C for 20 minutes, clearing of organic compounds by washing with methanol, oxidation of organics with hydrogen peroxide. The mineral IR spectroscopy characterization results showed the absence of organic compounds both before and after the treatments. Therefore, untreated MgO was used. The MgO used had a specific surface area of 32.89 $m^2 g^{-1}$ as measured by BET nitrogen adsorption isotherms (Sorptomatic 1990).

Batch adsorption isotherms were obtained by mixing 45 mg of MgO with 1.5 ml of stock solution with different initial concentration of nucleobase (0.1–30 mM) in sterile 2 ml Eppendorf tubes. These were suspended by vortex and agitated in an end-over-end shaker for about 24 hours at room temperature (~25 °C); this time is largely sufficient to reach equilibrium as established in the preliminary kinetic experiments (see Results section). After the adsorption process, the suspensions were centrifuged for 10 minutes at 15 000 rpm with a Hettich Zentrifugen Mikro 200 to obtain liquid–solid phase separation. Supernatant aliquots were collected, diluted and analysed by UV spectrophotometer and the amount of nucleobase adsorbed in equilibrium with the mineral was calculated by subtracting the amount of nucleobase in the supernatant from the total amount of nucleobase initially added. The supernatant solutions pH measured after equilibrium adsorption is about 10 in each case, due to the basicity of MgO.

Desorption experiments were performed as follows: the complexes formed after equilibrium adsorption were washed by resuspending the centrifuged pellets in 1.5 ml of water and

https://doi.org/10.1017/S1473550412000444 Published online by Cambridge University Press

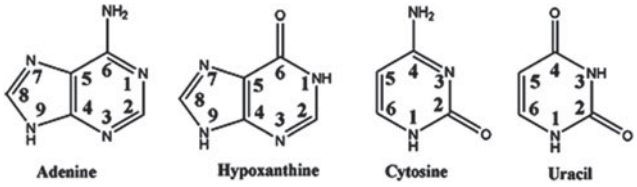

Fig. 1. Scheme of the nucleobases adenine, hypoxanthine, cytosine and uracil.

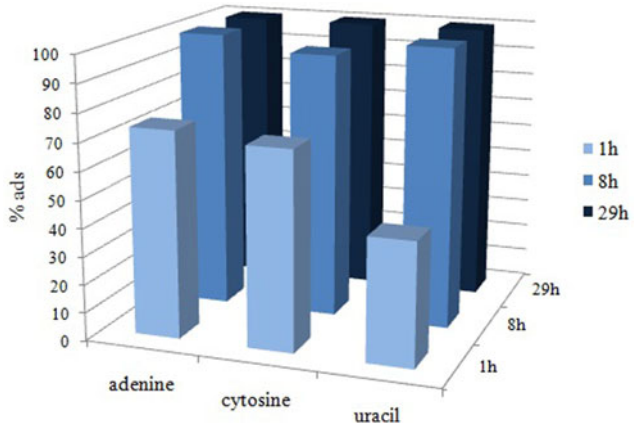

Fig. 2. Adsorption kinetics of adenine, cytosine and uracil onto MgO: relative percentage of adsorption versus time for three time steps: 1 hour, 8 hours and 29 hours.

the suspensions were shaken in an end-over-end shaker for about 30 minutes. After the washing time the suspensions were recentrifuged for 10 minutes at 15000 rpm and aliquots of supernatants were analysed by UV spectrophotometer to know the quantity of desorbed nucleobase. The washing cycles were repeated until no variations in the quantity of desorbed nucleobase were measured.

Data analyses were performed using the software MATLAB. For the quantitative analysis of UV spectra, we used the external standard method (ESTD) calibration procedure, to realize calibration curves that correlate the concentration of nucleobase solutions with the peak area in the UV spectra, through the Lambert–Beer law.

Table 1. *Adsorption isotherm experimental data for the nucleobases adenine, cytosine and uracil, and hypoxanthine adsorbed onto MgO at 298 K (nucleobase adsorbed moles are normalized on the surface area of the mineral)*

Initial nucleobase concentration (mM)	C_{eq} (mM)	n_{ads}/A_s (μmol m^{-2})	% ads
Adenine–MgO complexes			
27	13.8 ± 0.5	9 ± 2	37.8
20	10.7 ± 0.1	7.9 ± 0.6	41.3
14	4.9 ± 0.1	6.4 ± 0.9	56.1
10	4.4 ± 0.3	5.5 ± 0.9	56.4
7	1.292 ± 0.008	4.6 ± 0.6	77.7
4	0.89 ± 0.09	4.3 ± 0.6	83.1
3	0.100 ± 0.001	2.4 ± 0.6	96
1	(6 ± 4) * 10^{-4}	0.88 ± 0.06	99.9
Cytosine–MgO complexes			
30	27.8 ± 0.1	2.5 ± 0.3	8.17
20	16.19 ± 0.07	1.9 ± 0.2	10.2
15	13.40 ± 0.05	1.5 ± 0.3	10.2
10	7.92 ± 0.02	1.2 ± 0.2	12.8
7	5.90 ± 0.08	1.1 ± 0.1	15.1
5	3.81 ± 0.06	0.69 ± 0.09	15.1
3	2.46 ± 0.03	0.62 ± 0.09	19.9
1	0.6712 ± 0.0005	0.24 ± 0.01	25.8
0.5	0.3270 ± 0.0005	0.130 ± 0.003	28.1
Uracil–MgO complexes			
27	15.1 ± 0.7	13 ± 3	45
20	9.3 ± 0.4	9.5 ± 0.9	50.2
15	5.92 ± 0.07	7.4 ± 0.4	55.2
10	2.9 ± 0.2	5 ± 1	64.3
7	2.04 ± 0.01	5.3 ± 0.2	71.8
5	1.38 ± 0.01	3.0 ± 0.1	68.4
3	0.79 ± 0.03	2.7 ± 0.1	77.1
1	0.0949	0.81 ± 0.02	89.4
0.5	0.0934	0.432 ± 0.009	91.9
0.1	0.03	0.084 ± 0.002	93.6
Hypoxanthine–MgO complexes			
30	19.0 ± 0.6	11 ± 3	35.8
20	11.0 ± 0.2	6 ± 1	34.8
15	7.3 ± 0.1	5 ± 1	40.9
10	4.30 ± 0.07	4.3 ± 0.9	49.7
8	4.05 ± 0.05	4 ± 1	50
5	1.73 ± 0.06	3.3 ± 0.9	65
3	0.58 ± 0.01	2.7 ± 0.8	81.9
1	0.0186	1.03 ± 0.09	98.2

Results

A scheme of the nucleobases investigated is shown in Fig. 1. Guanine was not investigated because of the difficulties in experimental preparation, due to its low solubility. Moreover, for its ability to form numerous hydrogen bonds, in solutions and in the solid state the intermolecular interactions between guanine molecules cause considerable distortions of almost all physico-chemical characteristics in comparison with those of free molecules (Sheina *et al.* 1987). Uracil was chosen instead of thymine because of its greater prebiotic importance in the RNA world (Shelley *et al.* 2007).

Preliminary kinetic experiments were performed to estimate the time needed to reach the steady-state adsorption of nucleobases onto MgO. Sequential time steps were chosen to investigate the kinetics of the adsorption process. At each time step during the adsorption process an aliquot of the supernatant was collected and analysed by UV spectrophotometer to determine the amount of adsorbed nucleobase. The results of the kinetic experiments indicate that the steady-state adsorption on MgO is approached after 8 hours for all the nucleobases (Fig. 2). Therefore, an adsorption time of 24 hours was chosen for the subsequent adsorption experiments.

Adsorption isotherm data are reported in Table 1. Langmuir-type isotherms were fitted to data (Fig. 3), assuming: rapid reversible equilibration of adsorption; equivalence of all surface sites, i.e. uniform surface of the mineral; enthalpy of adsorption independent of coverage; not cooperativeness in the

https://doi.org/10.1017/S1473550412000444 Published online by Cambridge University Press

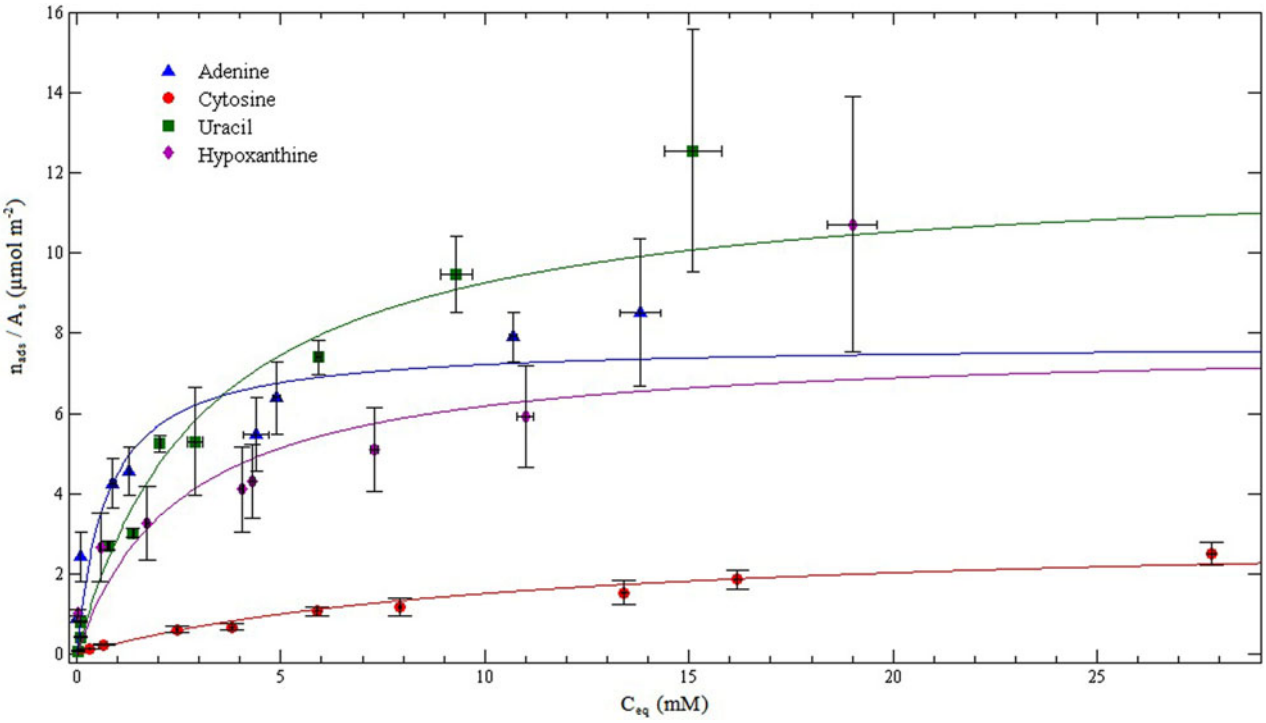

Fig. 3. Langmuir adsorption isotherm curves weighted fit for adenine (blue triangles), cytosine (red circles), uracil (green squares) and hypoxanthine (violet diamonds) adsorbed onto MgO at 298 K.

adsorption process, i.e. adsorbed molecules do not interact; and saturability of specific localized surface sites so that the saturation coverage corresponds to complete occupancy of these sites and at the maximum adsorption only a monolayer is formed (Atkins & de Paul 2002). The Langmuir isotherm model is represented by the equation: $n_{ads}/m_{mineral} = KbC_{eq}/(1 + KC_{eq})$, where $n_{ads}/m_{mineral}$ is the nucleobase adsorbed moles normalized on mineral mass, C_{eq} is the solute concentration in the aqueous phase at equilibrium, K is the Langmuir equilibrium adsorption constant, related to the enthalpy of adsorption, b is the amount of the solute per unit of adsorbent mass necessary to complete the monolayer. The best-fit values of K and b are reported in Table 2.

Desorption experiments were conducted to investigate the reversibility of the adsorption process (see Materials and methods section). The nucleobases desorption data are reported in Table 3 and the nucleobases desorbed percentages versus the elution volume are plotted in Figs. 4–6. In the case of cytosine–MgO complexes, within the experimental uncertainty, we observed a complete desorption.

Even if the washed nucleobases did not show changes in the UV-Vis spectrum, to verify possible alterations of the nucleobases catalysed by the mineral, high-performance liquid chromatography – mass spectrometry (HPLC-MS) analyses were performed using a Shimadzu instrument LCMS 2020 (C8 column, PDA detector, ESI source, quadrupole mass analyser). Analysis of results do not show evidence of formation of degradation products as a consequence of adsorption on MgO (data not shown).

Table 2. *Values of K, the Langmuir equilibrium adsorption constant, and b, the amount of the solute per unit of adsorbent mass necessary to complete the monolayer, derived from the Langmuir adsorption isotherm best-fit curves for adenine, cytosine, uracil and hypoxanthine adsorbed onto MgO at 298 K*

Sample	K (M^{-1})	b (mol g^{-1})
Adenine–MgO complexes	$(1 \pm 1)\cdot 10^3$	$(4 \pm 7)\cdot 10^{-4}$
Cytosine–MgO complexes	$(1.0 \pm 0.3)\cdot 10^2$	$(1.0 \pm 0.4)\cdot 10^{-4}$
Uracil–MgO complexes	$(3.0 \pm 0.9)\cdot 10^2$	$(4 \pm 2)\cdot 10^{-4}$
Hypoxanthine–MgO complexes	$(3 \pm 5)\cdot 10^2$	$(3 \pm 8)\cdot 10^{-4}$

Discussion

Comparison of the Langmuir adsorption isotherms for nucleobases adsorbed onto MgO at 298 K shows that the amount of solute per unit of adsorbent mass necessary to complete the monolayer onto MgO follows this order: uracil>hypoxanthine ~ adenine>cytosine. From the equilibrium adsorption constants we can observe that the adsorption process is thermodynamically more favourable for adenine than uracil and hypoxanthine, and after all cytosine. Therefore, the nucleobases adsorption order onto MgO is: adenine > uracil ⩾ hypoxanthine > cytosine. This is also the affinity order of nucleobases for MgO; in fact, as can be seen from the adsorption isotherms, in the adenine case the maximum adsorption is reached at lower concentrations, even if the amount of adenine adsorbed at saturation is less

https://doi.org/10.1017/S1473550412000444 Published online by Cambridge University Press

Table 3. *Desorption experimental data of adenine, uracil and hypoxanthine from MgO*

Elution volume (ml)	n_{des}/A_s (μmol m^{-2})	% des
MgO + A 20 mM		
0	0	0
1.5	2.7 ± 0.1	34 ± 4
3	3.9 ± 0.2	50 ± 6
4.5	4.7 ± 0.2	59 ± 7
6	5.5 ± 0.6	70 ± 10
7.5	5.8 ± 0.6	70 ± 10
MgO + A 10 mM		
0	0	0
1.5	1.49 ± 0.06	27 ± 6
3	2.31 ± 0.09	42 ± 9
4.5	2.77 ± 0.09	50 ± 10
6	3.10 ± 0.09	60 ± 10
7.5	3.37 ± 0.09	60 ± 10
MgO + A 5 mM		
0	0	0
1.5	0.53 ± 0.02	12 ± 2
3	0.91 ± 0.03	21 ± 4
4.5	1.19 ± 0.03	28 ± 5
6	1.43 ± 0.06	33 ± 6
7.5	1.61 ± 0.06	38 ± 7
MgO + A 1 mM		
0	0	0
1.5	$(6 \pm 3)\cdot10^{-4}$	0.07 ± 0.04
3	$(1.5 \pm 0.9)\cdot10^{-3}$	0.2 ± 0.2
4.5	$(2 \pm 1)\cdot10^{-3}$	0.3 ± 0.2
6	$(4 \pm 1)\cdot10^{-3}$	0.4 ± 0.2
7.5	$(5 \pm 2)\cdot10^{-3}$	0.5 ± 0.2
MgO + U 20 mM		
0	0	0
1.5	2.9 ± 0.3	31 ± 6
3	4.3 ± 0.3	46 ± 8
4.5	5.5 ± 0.3	59 ± 9
6	6.4 ± 0.3	70 ± 10
7.5	7.0 ± 0.3	70 ± 10
MgO + U 10 mM		
0	0	0
1.5	1.2 ± 0.2	23 ± 9
3	2.1 ± 0.3	40 ± 20
4.5	2.7 ± 0.3	50 ± 10
6	3.3 ± 0.3	60 ± 20
7.5	3.6 ± 0.3	70 ± 20
MgO + U 5 mM		
0	0	0
1.5	0.74 ± 0.02	25 ± 1
3	1.25 ± 0.03	41 ± 3
4.5	1.58 ± 0.06	52 ± 3
6	1.79 ± 0.09	60 ± 5
7.5	1.98 ± 0.09	66 ± 5
MgO + U 1 mM		
0	0	0
1.5	0.056 ± 0.001	6.9 ± 0.2
3	0.13 ± 0.03	16.3 ± 0.8
4.5	0.20 ± 0.03	24 ± 1
6	0.26 ± 0.06	32 ± 1
7.5	0.30 ± 0.06	38 ± 2
MgO + U 0.5 mM		
0	0	0
1.5	0.0347 ± 0.0006	8.02 ± 0.02
3	0.067 ± 0.001	15.58 ± 0.04
4.5	0.098 ± 0.002	22.73 ± 0.05
6	0.127 ± 0.003	29.43 ± 0.07
7.5	0.152 ± 0.003	35.65 ± 0.08
MgO + U 0.1 mM		
0	0	0
1.5	$(6.3 \pm 0.1)\cdot10^{-3}$	7.46
3	$(1.15 \pm 0.02)\cdot10^{-2}$	13.6
4.5	$(1.67 \pm 0.03)\cdot10^{-2}$	19.73
6	$(2.16 \pm 0.06)\cdot10^{-2}$	25.87
7.5	$(2.61 \pm 0.06)\cdot10^{-2}$	30.93
MgO + HY 20 mM		
0	0	0
1.5	1.61 ± 0.03	27 ± 2
3	2.22 ± 0.06	37 ± 3
4.5	2.64 ± 0.06	44 ± 4
6	2.92 ± 0.09	49 ± 5
7.5	3.16 ± 0.09	53 ± 5
9	3.34 ± 0.09	57 ± 5
MgO + HY 1 mM		
0	0	0
1.5	$(1.49 \pm 0.03)\cdot10^{-2}$	1.4 ± 0.1
3	$(2.92 \pm 0.06)\cdot10^{-2}$	2.8 ± 0.2
4.5	$(4.41 \pm 0.09)\cdot10^{-2}$	4.2 ± 0.3
6	$(5.8 \pm 0.1)\cdot10^{-2}$	5.6 ± 0.4
7.5	$(7.3 \pm 0.1)\cdot10^{-2}$	7.0 ± 0.5
9	$(8.7 \pm 0.2)\cdot10^{-2}$	8.3 ± 0.6

than the uracil one. We can deduce that the number of available sites on MgO for the adsorption of adenine is lower than for uracil and that for cytosine is lower than for adenine. The possible interpretation for the observed adsorption order onto MgO may be ascribed to the molecular differences in the van der Waals surface area of the nucleobases, i.e. uracil size (pyrimidine) is smaller than the hypoxanthine and adenine ones (purine), so the number of available sites on MgO for the adsorption of adenine and hypoxanthine is lower than for uracil. Nevertheless, in the case of cytosine, the lower adsorption with respect to the other nucleobases suggests the involvement of electrostatic interactions with MgO. Generally, the adsorption of organic molecules onto mineral surfaces is a complex thermodynamic process, in which the resultant orientation of the molecules is the most energetically favourable depending on the synergy of the different types of specific and non-specific interactions (e.g. ionic, covalent, van der Waals, hydrogen-bonding interactions, solvophobic effects and coordination bonding). Therefore, all possible factors may be taken into account to explain the observed adsorption results. In particular, the solution pH is a fundamental parameter that influences the nucleobases solubility, the keto-enol tautomerization equilibrium (Kochetkov & Budovskii 1972) and especially the charge of nucleobases, due to the possibility of nucleobases to undergo protonation or deprotonation depending on the solution pH, acquiring positive or negative charges and consequently influencing the adsorption for the involvement of electrostatic interactions. In our experimental conditions, the equilibrium solution pH is about 10 in all cases due to the basicity of MgO, which implies that during the adsorption process, adenine, uracil and hypoxanthine are largely in the anionic form, while cytosine is neutral, as can be deduced from the nucleobases pK_a (Dawson *et al.* 1986). The point of zero charge for MgO is ∼12 (Schramm 2005), therefore at pH 10 the surface of MgO should be positively charged, favouring the adsorption of the anionic nucleobases for the involvement of strong ionic interactions, in addition to the electrostatic interactions that may take place via the π electrons of the aromatic rings and/or via the lone pair

https://doi.org/10.1017/S1473550412000444 Published online by Cambridge University Press

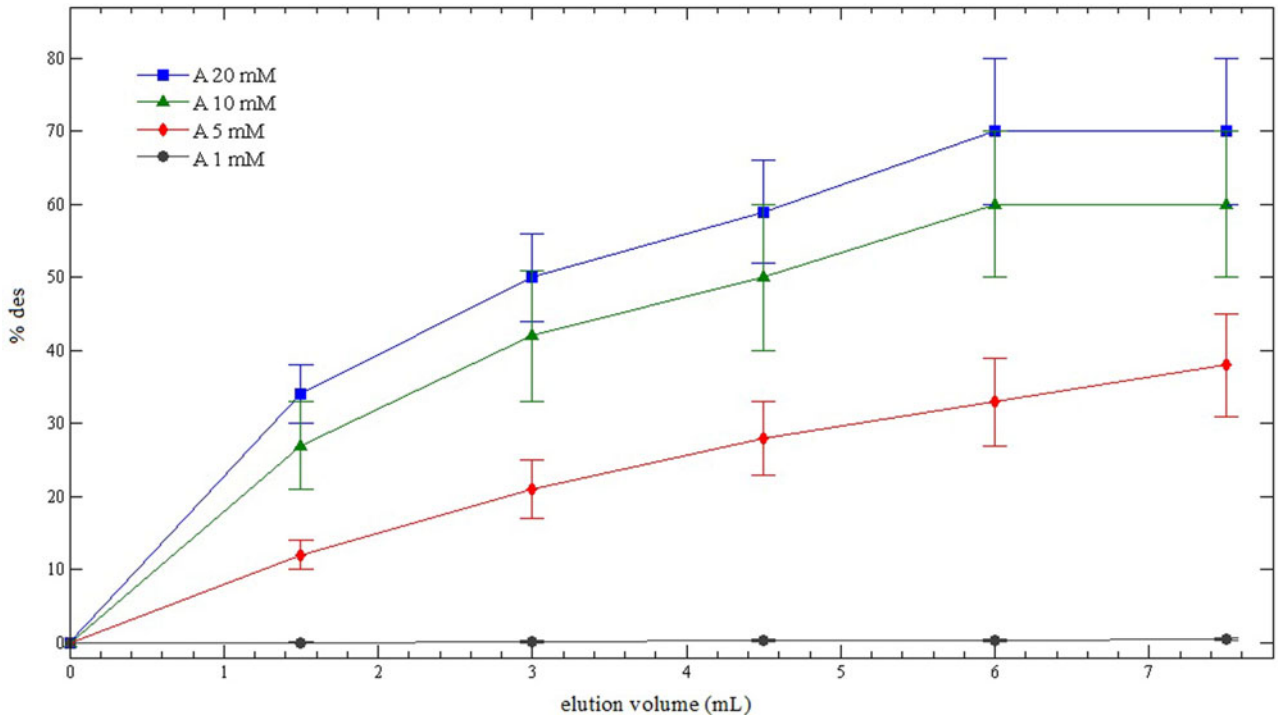

Fig. 4. Desorption curve for adenine–MgO complexes: MgO + A 20 mM (blue squares), MgO + A 10 mM (green triangles), MgO + A 5 mM (red diamonds) and MgO + A 1 mM (grey circles).

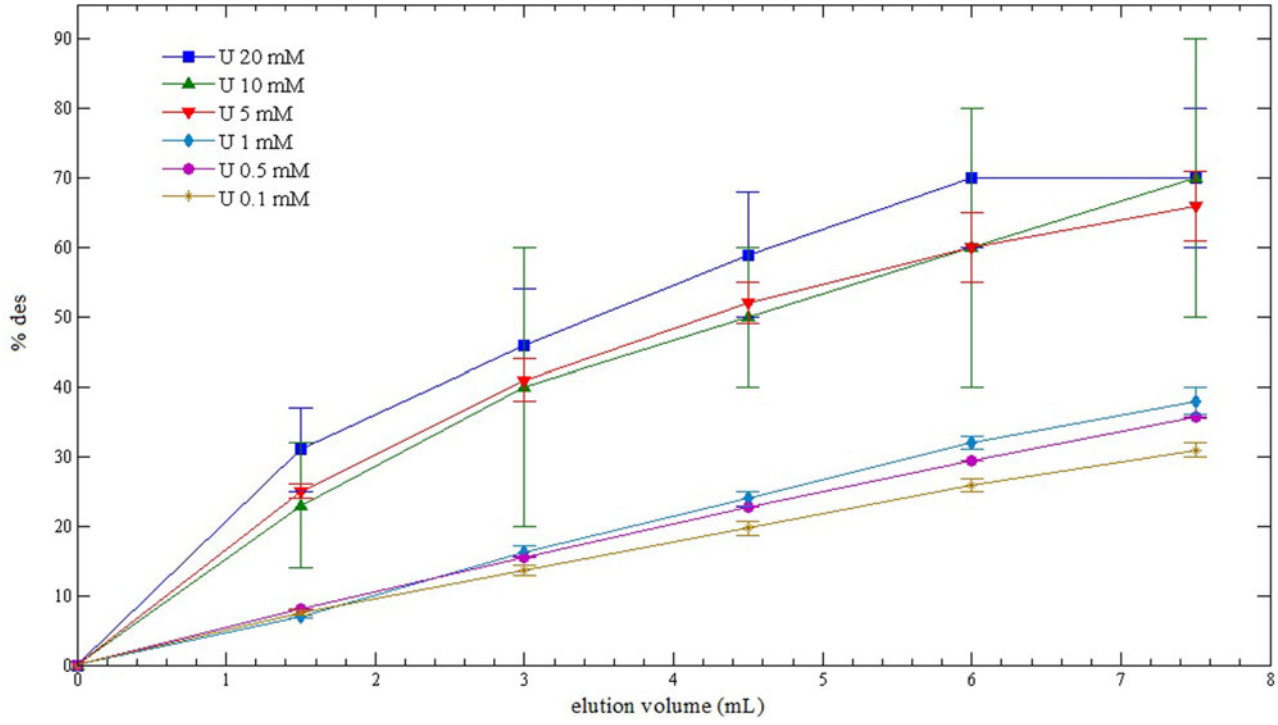

Fig. 5. Desorption curve for uracil–MgO complexes: MgO + U 20 mM (dark blue squares), MgO + U 10 mM (green up-triangles), MgO + U 5 mM (red down-triangles), MgO + U 1 mM (light blue diamonds), MgO + U 0.5 mM (violet circles) and MgO + U 0.1 mM (light brown stars).

of electrons on N and O atoms of the nucleobases. Moreover, the low adsorption of cytosine may be attributed also to its higher solubility in water (Budavari 1996). A correspondence between the adsorption order of nucleobases onto MgO, and the hydrophobicity order of nucleobases can also be noted (Shih *et al.* 1998): adenine > uracil > hypoxanthine ⩾ cytosine,

https://doi.org/10.1017/S1473550412000444 Published online by Cambridge University Press

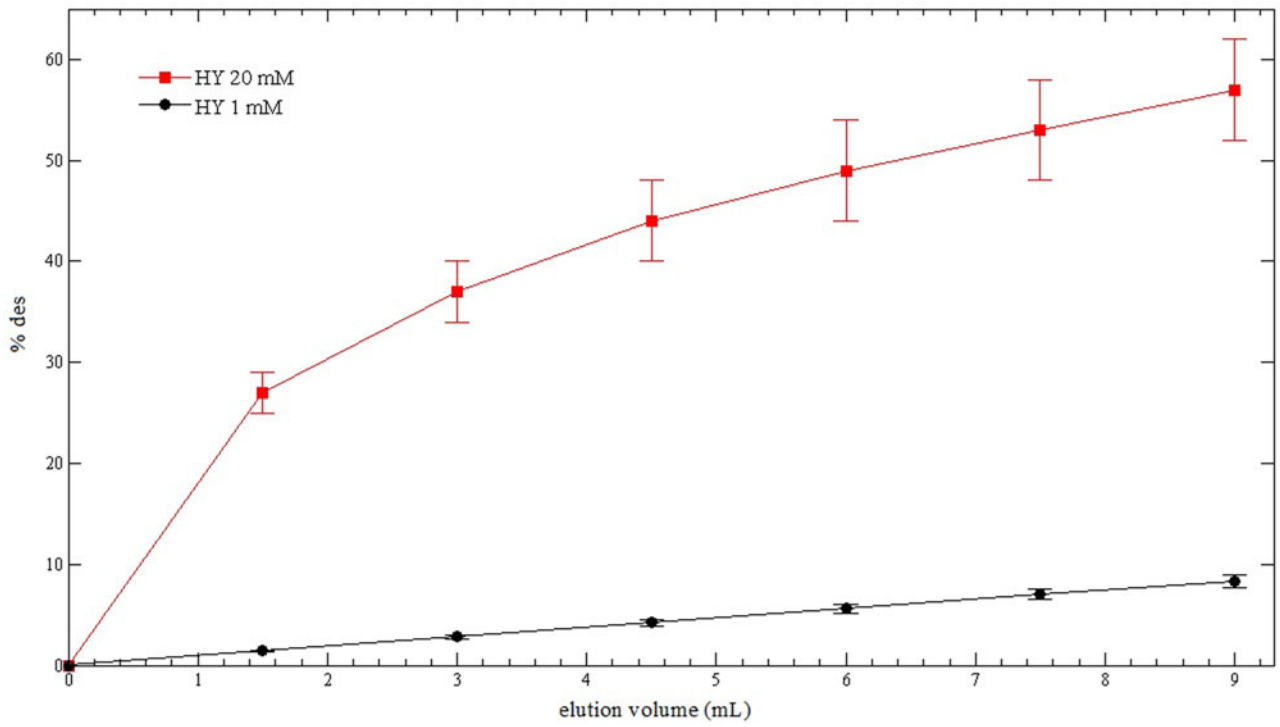

Fig. 6. Desorption curve for hypoxanthine–MgO complexes: MgO + HY 20 mM (red squares) and MgO + HY 1 mM (black circles).

indicating that hydrophobic effect also contributes to the adsorption process, favouring the passage of the most hydrophobic nucleobases from the aqueous solution to the mineral surface. This suggests also the involvement of hydrophobic interactions between the aromatic rings of nucleobases and the mineral. However, the chemistry of the surface of MgO is certainly dominated by its basicity, due to the basic O^{2-} ions and $-OH$ groups on the surface, and Brønsted acids may chemisorb on MgO forming carbanions and $-OH$ groups, adsorbates may react dissociatively with the surface ion pairs (Gates 1992). The reactivity of the most common surface of MgO powder, the (100) face, to adsorbates appears to be directly related to the acidity of the molecule. The lower its pK_a the more molecules react with the single-crystal MgO surface. Dissociative chemisorptions are often irreversible. Instead, the desorption studies show a great reversibility in the adsorption process of nucleobases on MgO for all nucleobases, and most of all for cytosine, which establishes very labile interactions with MgO resulting in a completely reversible process. Coherently, cytosine adsorbs to a minor extent than adenine, uracil and hypoxanthine onto MgO, and desorbs to a greater extent. The nucleobases desorption order from MgO can be assessed: cytosine > adenine ⩾ uracil > hypoxanthine; it follows that the percentage of desorbed nucleobases varies depending on the specific interactions of the different nucleobases with the mineral. Even if the distinction between physisorption and chemisorption is somewhat arbitrary and in many cases intermediate or more complex processes occur, we can assess that in the case of nucleobases onto MgO, a physisorption process occurs predominantly. It is plausible to hypothesize a molecular mechanism of adsorption in which the anionic nucleobases do not directly bind to the surface of MgO but they approach to the hydroxylated surface, giving rise to an outer sphere surface complex dominated by weaker long-range interactions. In fact, water might preferentially give dissociative chemisorption, being in excess respect to nucleobases, determining the hydroxylation of the surface of MgO. The hydroxyl groups on the surface of MgO are the most important sites for surface interactions and, existing in acidic or basic forms, can act as acids or bases depending of the pH of the solution. At the equilibrium pH 10 the surface hydroxyl groups should be in the acidic form and might interact with the deprotonated nucleobases adenine, uracil and hypoxanthine through ionic interactions. This kind of interactions between nucleobases and the surface of the mineral may be largely reversible.

Conclusions

Present work shows that MgO is a good adsorbent for nucleobases. This observation supports hypothesis that metal oxides may be responsible of concentrating biomolecules in prebiotic conditions, probably protecting them and favouring chemical reactions towards more complex species. Moreover, the observed differential adsorption of nucleobases on this mineral could be prebiotically relevant, influencing the composition of a possible primordial genetic architecture. However, the adsorption properties of nucleobases are very dependent on the mineral characteristics and the nucleobases adsorption order may change greatly with different minerals.

https://doi.org/10.1017/S1473550412000444 Published online by Cambridge University Press

For instance, Cleaves *et al.* (2010) observed a much higher adsorption of adenine and cytosine with respect to hypoxanthine and uracil onto rutile (TiO_2). Sowerby *et al.* (2001a) showed that the adsorption of nucleobases on crystalline graphite follows this series: guanine > adenine > hypoxanthine > thymine > cytosine > uracil. In the last case, the weaker adsorption of pyrimidines is supposed to strengthen the hypothesis of purine-only genetic systems (Crick 1968; Wächtershauser 1988). Nevertheless the nucleobases adsorption order onto MgO is completely different and uracil shows the highest adsorption at saturation. Therefore, it is difficult to define a universal adsorption mechanism of nucleobases onto inorganic matrices, responsible of the origin of a primordial genetic coding machinery, which would have been reflected in the modern biochemistry. The passage from geochemistry to biochemistry probably resulted from the combination of multiple complex phenomena between organic and inorganic systems, and studying how organic molecules interact with minerals may be only a step forward in the comprehension of the unsolved question of the origin of life.

Acknowledgements

We thank F. Montagnaro of the University of Naples Federico II, for the BET measurements. This work was supported by Italian Space Agency (ASI) grant I/060/10/0.

References

Atkins, P. & de Paul, J. (2002). *Physical Chemistry*, 7th edn. Oxford University Press, Oxford.
Barber, D.J. & Scott, E.R.D. (2002). *Proc Natl Acad Sci USA* **99**, 6556–6561.
Barks, H.L., Buckley, R., Grieves, G.A., Di Mauro, E., Hud, N.V. & Orlando, T.M. (2010). *ChemBioChem*. **11**, 1240–1243.
Bebié, J. & Schoonen, M.A.A. (2000). *Geochem. Trans*. **8**, DOI:10.1039/b005581f.
Bernal, J.D. (1951). *The Physical Basis of Life*. Routledge and Kegan Paul, London.
Brucato, J.R., Strazzulla, G., Baratta, G.A., Rotundi, A. & Colangeli, L. (2006). *Orig. Life Evol. Biosph*. **36**(5–6), 451–457.
Budavari, S. (1996). *The Merck Index*, 12th edn, Merck and Co. Inc., Rahway, NJ.
Cleaves, H.J. II, Jonsson, C.M., Jonsson, C.L., Sverjensky, D.A. & Hazen, R.M. (2010). *Astrobiology* **10**(3), 311–323.
Cohn, C.A., Hansson, T.K., Larsson, H.S., Sowerby, S.J. & Holm, N.G. (2001). *Astrobiology* **1**(4), 477–480.
Crick, F.H.C. (1968). *J. Mol. Biol*. **38**, 367–379.
Cullen, D.C. & Sims, M.R. (2007). Life detection within planetary exploration: context for biosensor and related bioanalytical technologies. In *Handbook of Biosensors and Biochips*, ed. Marks, R.S., Cullen, D.C., Karube, I., Lowe, C.R. & Weetall, H.H., pp. 1237–1256. John Wiley and Sons, Chichester, UK.
Dawson, R.M.C., Elliott, D.C., Elliott, W.H. & Jones, K.M. (1986). *Data for Biochemical Research*, 3rd edn, Oxford University Press, Oxford.
Direito, S.O.L., Marees, A. & Roeling, W.F.M. (2012). *Fed. Eur. Microbiol. Soc*. **81**, 111–123.
Downs, R.T. & Hazen, R.M. (2004). *J. Mol. Catal. A: Chem*. **216**, 273–285.
Edelwirth, M., Freund, J., Sowerby, S.J. & Heckl, W.M. (1998). *Surf. Sci*. **417**, 201–209.
Ertem, G. (2004). *Orig. Life Evol. Biosph*. **34**, 549–570.
Ferris, J.P. (1992). In *Marine Hydrothermal Systems and the Origin of Life*, ed. Holm, N.G., Kluwer, Dordrecht, The Netherlands.
Gates, B.C. (1992). *Catalytic Chemistry*, John Wiley and Sons Inc., New York.
Gibbs, D., Lohrmann, R. & Orgel, L.E. (1980). *J. Mol. Evol*. **15**, 347–354.
Gilbert, W. (1986). *Nature* **319**, 618.
Hazen, R.M. (2006). *Am. Mineral*. **91**, 1715–1729.
Hazen, R.M. & Sholl, D.S. (2003). *Nature Mater*. **2**, 367–374.
Hazen, R.M. & Sverjensky, D.A. (2010). *Cold Spring Harb. Perspect. Biol*. **2**, a002162.
Hazen, R.M., Filley, T.R. & Goodfriend, G.A. (2001). *Proc. Natl Acad. Sci. USA* **98**(10), 5487–5490.
Heckl, W.M., Smith, D.P.E., Binnig, G., Klagges, H., Hänsch, T.W. & Maddocks, J. (1991). *Proc. Natl Acad. Sci. USA* **88**, 8003–8005.
Holm, N.G. (2012). *Geobiology*, **10**(4), 269–279.
Kochetkov, N. & Budovskii, E.I. (1972). *Organic Chemistry of Nucleic Acids*, Plenum Press, New York.
Komiyama, M., Gu, M., Shimaguchi, T., Wu, H.M. & Okada, T. (1998). *Appl. Phys. A: Mater. Sci. Process*. **66**, S635–S637.
Lahav, N. (1999) *Biogenesis: Theories of Life's Origin*. Oxford University Press, New York, p. 259.
Lahav, N. & Chang, S. (1976). *J. Mol. Evol*. **8**, 357–380.
Levy, M., Miller, S.L., Brinton, K. & Bada, J.L. (2000). *Icarus* **145**, 609–613.
Lorenz, M.G. & Wackernagel, W. (1994). *Microbiol. Rev*. **58**, 563–602.
Luther, A., Brandsch, R. & von Kiedrowski, G. (1998). *Nature* **396**, 245–248.
Miller, S.L. (1987). *Cold Spring Harb. Symp. Quant. Biol*. **52**, 17–27.
Ming, D.W. *et al.* (2006). *J. Geophys. Res*. **111**, E02S12 (doi: 10.1029/2005JE002560).
Parnell, J. *et al.* (2007). *Astrobiology* **7**(4), 578–604.
Peeters, Z., Quinn, R., Martins, Z., Sephton, M.A., Becker, L., van Loosdrecht, M.C.M., Brucato, J.R., Grunthaner, F. & Ehrenfreund, P. (2009). *Int. J. Astrobiol*. **8**(4), 301–315.
Plekan, O., Feyer, V., Šutara, F., Skála, T., Švec, M., Cháb, V., Matolín, V. & Prince, K.C. (2007). *Surf. Sci*. **601**, 1973–1980.
Podlech, J. (2001). *Cell. Mol. Life Sci*. **58**, 44–60.
Pucci, A., Branciamore, S., Casarosa, M., Acqui, L.P.D. & Gallori, E. (2010). *J. Cosmol*. **10**, 3398–3407.
Saladino, R., Crestini, C., Costanzo, G., Negri, R. & Di Mauro, E. (2001). *Bioorg. Med. Chem*. **9**(5), 1249–1253.
Saladino, R., Ciambecchini, U., Crestini, C., Costanzo, G., Negri, R. & Di Mauro, E. (2003). *ChemBioChem*. **4**(6), 514–521.
Saladino, R., Crestini, C., Ciambecchini, U., Ciciriello, F., Costanzo, G. & Di Mauro, E. (2004). *ChemBioChem*. **5**(11), 1558–1566.
Saladino, R., Crestini, C., Costanzo, G. & Di Mauro, E. (2005a). *Top. Curr. Chem*. **259**, 29–68.
Saladino, R., Crestini, C., Neri, V., Brucato, J.R., Colangeli, L., Ciciriello, F., Di Mauro, E. & Costanzo, G. (2005b). *ChemBioChem*. **6**, 1–7.
Saladino, R., Brucato, J.R., de Sio, A., Botta, G., Pace, E. & Gambicorti, L. (2011). *Astrobiology* **11**, 815–824.
Scappini, F., Casadei, F., Zamboni, R., Franchi, M., Gallori, E. & Monti, S. (2004). *Int. J. Astrobiol*. **3**(1), 17–19.
Schoonen, M., Smirnov, A. & Cohn, C. (2004). *Ambio* **33**(8), 539–551.
Schramm, L.L. (2005). *Emulsions, Foams, and Suspensions*, Wiley-VCH, New York.
Sheina, G.G., Stepanian, S.G., Radchenko, E.D. & Blagoi, Yu. P. (1987). *J. Mol. Struct*. **158**, 275–292.
Shelley, D.C., Smith, E. & Morowitz, H.J. (2007). *Bioorg. Chem*. **35**, 430–443.
Shih, P., Pedersen, L.G., Gibbs, P.R. & Wolfenden, R. (1998). *J. Mol. Biol*. **280**, 421–430.
Sholl, D.S. & Gellman, A.J. (2009). *AIChE J*. **55**(10), 2484–2490.
Singh, H.K., Saquib, M., Haque, M.M. & Muneer, M. (2007). *J. Hazard. Mater*. **142**, 425–430.
Sowerby, S.J. & Heckl, W.M. (1998). *Orig. Life Evol. Biosph*. **28**, 283–310.
Sowerby, S.J. & Petersen, G.B. (1997). *J. Electroanal. Chem*. **433**, 85–90.

Sowerby, S.J. & Petersen, G.B. (1999). *Orig. Life Evol. Biosph.* **29**, 597–614.
Sowerby, S.J., Heckl, W.M. & Petersen, G.B. (1996). *J. Mol. Evol.* **43**, 419–424.
Sowerby, S.J., Edelwirth, M. & Heckl, W.M. (1998). *J. Phys. Chem. B* **102**, 5914–5922.
Sowerby, S.J., Stockwell, P.A., Heckl, W.M. & Petersen, G.B. (2000). *Orig. Life Evol. Biosph.* **30**, 81–99.
Sowerby, S.J., Cohn, C.A., Heckl, W.M. & Holm, N.G. (2001a). *Proc. Natl Acad. Sci. USA* **98**(3), 820–822.
Sowerby, S.J., Mörth, C.-M. & Holm, N.G. (2001b). *Astrobiology* **1**(4), 481–487.
Sowerby, S.J., Petersen, G.B. & Holm, N.G. (2002). *Orig. Life Evol. Biosph.* **32**, 35–46.
Stotzky, J.V., Gallori, E. & Khanna, M. (1996). *Molecular Microbial Ecology Manual*, eds Akkermans, A.D.I., Van Elsas, J.D. & De Brujin F.J., pp. 1–28. Kluwer Academic, Dordrecht, The Netherlands.
Tao, N.J., DeRose, J.A. & Lindsay, S.M. (1993). *J. Phys. Chem.* **97**, 910–919.
Tao, N.J. & Shi, Z. (1994). *J. Phys. Chem.* **98**, 1464–1471.
Valocchi, A.J. (1985). *Water Resour. Res.* **21**(6), 808–820.
Wächtershauser, G. (1988). *Proc. Natl Acad. Sci. USA* **85**, 1134–1135.
Winter, D. & Zubay, G. (1995). *Orig. Life Evol. Biosph.* **25**, 61–81.